SANDIA REPORT
SAND2007-1905
Unlimited Release
Printed March 2007

Development of Platinum-Loaded Y-Type Zeolite Catalysts for High Efficiency Conversion of Biomass-Derived Carbohydrates to Hydrogen

Justin Monroe

Prepared by
Sandia National Laboratories
Albuquerque, New Mexico 87185 and Livermore, California 94550

Sandia is a multiprogram laboratory operated by Sandia Corporation,
a Lockheed Martin Company, for the United States Department of Energy's
National Nuclear Security Administration under Contract DE-AC04-94AL85000.

Issued by Sandia National Laboratories, operated for the United States Department of Energy by Sandia Corporation.

Available to DOE and DOE contractors from
U.S. Department of Energy
Office of Scientific and Technical Information
P.O. Box 62
Oak Ridge, TN 37831

Telephone: (865) 576-8401
Facsimile: (865) 576-5728
E-Mail: reports@adonis.osti.gov
Online ordering: http://www.osti.gov/bridge

Available to the public from
U.S. Department of Commerce
National Technical Information Service
5285 Port Royal Rd.
Springfield, VA 22161

Telephone: (800) 553-6847
Facsimile: (703) 605-6900
E-Mail: orders@ntis.fedworld.gov
Online order: http://www.ntis.gov/help/ordermethods.asp?loc=7-4-0#online

SAND2007-1905
Unlimited Release
Printed March 2007

Development of Platinum-Loaded Y-Type Zeolite Catalysts for High Efficiency Conversion of Biomass-Derived Carbohydrates to Hydrogen

Justin Monroe
New Mexico Institute of Mining and Technology
Department of Materials and Metallurgical Engineering
801 Leroy Place
Socorro, NM 87801-4796

Abstract

Production of hydrogen (H_2) from biomass and organic wastes is considered an effective approach to mitigating the environmental problems caused by pollutant emissions from fossil fuel combustion and allaying our dependence on the limited oil reserves. However, current technological inefficiencies render such biomass utilization economically unviable. A promising alternative to realizing the goal of hydrogen from renewable sources is to convert biomass-derived carbohydrates to H_2. To make the process economically attractive, catalysts with higher performance and low cost need to be developed. This research aims to develop new zeolite-based catalysts for highly efficient liquid phase conversion of carbohydrates to H_2. Particulate platinum-loaded Y-type zeolite (Pt/NaY) catalysts have been synthesized, characterized, and evaluated for H_2 production from methanol. The catalysts were also tested for liquid phase reforming of ethanol and glucose to hydrogen.

Acknowledgements

The work discussed in this report was supported by a Campus Executive Laboratory Directed Research and Development (LDRD) research project. The author wishes to acknowledge Sandia National Laboratories for this support. I would like to thank HNEI/DOE for also support and funding this research. I'd like to thank Dr. Junhang Dong for guidance he has given me with the project, and knowledge in life he has given me as a friend. I would like to thank Dr. Deidra Hirschfeld for her guidance with the project and help in the classes. I would like to thank Dr. Dan Doughty of Sandia National Laboratories for his insightful discussions on the projects. I would like to thank Dr. Ping Lu for his valuable comments on material characterizations. I would like to thank Dr. Xuehong Gu for his continual help during the project. I would like to thank Dr. Zhong Tang, Mr. Paul Quintana, and Dr. Liangxiaong Li for their help with the catalytic reaction experiments and material characterizations. I would like to thank Nelia Dunbar for her help with microprobe analysis. I would like to thank Chris McKee for his help with running x-ray diffraction analysis of the sample. Finally, I would like to thank the rest of the research group and my friends not mentioned above for their support throughout my graduate research.

Summary

Production of hydrogen (H_2) from biomass and organic wastes is considered an effective approach to mitigating the environmental problems caused by pollutant emissions from fossil fuel combustion and allaying our dependence on the limited oil reserves. However, current technological inefficiencies render such biomass utilization economically unviable. A promising alternative to realizing the goal of hydrogen from renewable sources is to convert biomass-derived carbohydrates to H_2. Recently, the γ-Al_2O_3 supported platinum (Pt/γ-Al_2O_3) catalysts have been successfully demonstrated for the liquid phase reforming of various carbohydrates into hydrogen at temperatures below 300^oC. However, the throughput of the catalytic conversion is low and the cost of the catalyst is high because of the high load of Pt metal, typically in a range of 3wt% - 5wt%. To make the process economically attractive, catalysts with higher performance and low cost need to be developed. This research aims to develop new zeolite-based catalysts for highly efficient liquid phase conversion of carbohydrates to H_2. Particulate platinum-loaded Y-type zeolite (Pt/NaY) catalysts have been synthesized, characterized, and evaluated for H_2 production from methanol. The catalysts were also tested for liquid phase reforming of ethanol and glucose to hydrogen. The catalytic performances of the Pt/NaY catalysts have been compared with that of the Pt/γ-Al_2O_3 catalysts reported in the literature as well as synthesized in this work. The Pt/NaY catalyst with a Pt load of 0.5 wt% was found to outperform the Pt/γ-Al_2O_3 catalysts with a Pt load of ~3 wt% for conversion of methanol to H_2. The Pt/NaY catalyst was demonstrated to be active for ethanol reforming in liquid phase, but incapable of catalyzing glucose because the ringed glucose molecules are too large to effectively transport into the zeolite pores (~0.7 nm diameter), where the Pt metal clusters locate. Results of this research indicate that the

transition metal-load Y-type zeolite catalysts have great potential for use in catalytic reforming of carbohydrates to H_2.

CONTENTS

LIST OF FIGURES

LIST OF TABLES

INTRODUCTION

Hydrogen is a clean energy carrier which can serve as an alternative to fossil fuels such as gasoline or diesel. Alternative sources of fuel are needed for two main reasons. The first is that there is a limited supply of petroleum in the world. In the future, an alternative supply of fuel will be necessary. Secondly, there are environmental concerns associated with combustion of fossil fuels that include the buildup of CO_2 and pollutants, such as NO_x and SO_x, in the atmosphere. As the world's economy continues to grow, consumption of fossil fuels will increase and so will the CO_2 buildup in the atmosphere. In 2000, the CO_2 level in the atmosphere rose above 370 parts per million by volume (ppmv). The highest recorded level from Greenland ice core data was 310 ppmv over the previous 240,000 years.[1] The high level of CO_2 and other greenhouse gases in the atmosphere is believed to be responsible for the global warming effect, which, if not controlled effectively, will result in catastrophic extreme climates, while the other pollutants have caused severe problems to the earth environment, agriculture, and human health.

Approximately two-thirds of oil used in the United States and half of the oil used worldwide is for transportation.[2] As more motor vehicles and highways are built in developing countries the demand for oil will grow. From 1992 to 2001, world oil production grew from 65.7 to 74.7 million barrels a day.[1] While these numbers may seem staggering, oil demand is expected to increase another 50 to 120 million barrels a day by 2015.[1] The current estimated oil reserve is expected to support the global consumption for less than forty years. Because of these predictions, tremendous research efforts have recently been made on finding alternative fuels, hydrogen in particular, and

developing fuel cells, the key technology for H_2-driven vehicles, to achieve low or zero emission and high efficiency of energy utilization. There are many types of fuel cells under research and development (e.g. proton exchange membrane fuel cells (PEMFC), solid oxide fuel cells, molten carbonate fuel cells etc.). Currently, almost all the fuel cells are powered by hydrogen. A PEMFC operates based on the following electrochemical reactions:

$$\text{Anode:} \qquad H_2 \xrightarrow{Catalyst} 2H^+ + 2e^-$$

$$\text{Cathode:} \qquad 2e^- + 2H^+ + \frac{1}{2}O_2 \xrightarrow{Catalyst} H_2O$$

As illustrated in Figure 1 below, hydrogen is ionized at the anode forming H^+ ions (protons) and electrons. The electrons pass through the outer circuit, providing the vehicle electrical power, while protons pass through the electrolyte to react with the oxygen at the cathode to form water. Thus, the only chemical product from the fuel cell is clean water. Fuel cell technology is thought of as a potential solution to the energy crisis and many environmental problems because it has much higher energy efficiency compared to the traditional internal combustion and thermal-based technologies.[3] Although hydrogen fuels do not produce CO_2, production of H_2 may involve CO_2 production as fossil fuels are currently the predominant sources for H_2 generation. It is highly desired that hydrogen can be generated by technologies free of CO_2 emission or reformed with CO_2 readily captured for sequestration so that the reduction of CO_2 emission can be maximized.

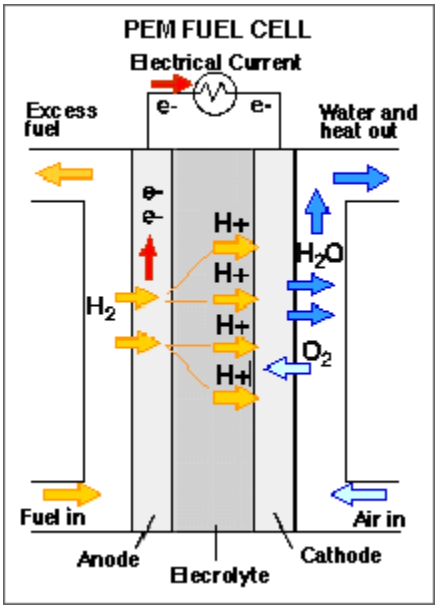

Figure 1. Operation mechanism of the proton exchange membrane (PEM) fuel cell.

CURRENT STATUS OF HYDROGEN PRODUCTION

Currently, hydrogen from fossil fuels, i.e. natural gas, oil, and coal, accounts for 95% of its total production in the United States with 90% coming from natural gas.[4] The state-of-the-art industrial technologies, i.e. steam-reforming of natural gas (methane), coal, and liquid petroleum gases, produce hydrogen that costs more than gasoline for the same amount of energy/power. In order to make the transition to the hydrogen economy, a cheap and efficient method must be developed for producing hydrogen. While great efforts are still being made to improve the steam-reforming technology to lower the H_2 cost, other methods of hydrogen production are being actively researched. These new methods include water electrolysis using electricity from solar or wind energy, gasification of coal, petroleum coke and biomass conversion with CO_2-capture, and thermochemical water splitting powered by high temperature nuclear or solar heat.[5]

Hydrogen from Steam Reforming

Hydrogen made from methane or coal is produced by the following catalytic reactions:

Natural gas:	$CH_4(g) + H_2O(g) \leftrightarrow 3H_2(g) + CO(g)$
Coal:	$C\ (s) + H_2O(g) \leftrightarrow H_2(g) + CO(g)$
Water-gas shift	$CO(g) + H_2O(g) \leftrightarrow H_2\ (g) + CO_2(g)$

These reactions are overall endothermic, requiring the input of heat by burning part of the natural gas or coal.[6] When looking for a method of hydrogen production, it is important to compare the amount of green house gases (GHG) produced for generating a unit amount of hydrogen. This is also called ‘well to wheels’ air pollutant emissions.

Hydrogen fuel cells are a clean and efficient technology in which the only byproduct is water. However, in the production of hydrogen from fossil fuels, CO_2 is produced. Figure 2 below shows the well to wheels production of air pollutant emissions for various types of vehicles and fuels.[7-12] As can be seen in the figure, there are a number of different methods which are better options in terms of emission reduction. However, the list of "better options" narrows down when cost considerations are accounted for. For instance, zero emission electrolytic hydrogen supply options such as wind, solar and nuclear energy are currently several times as expensive as hydrogen produced from natural gas.[5]

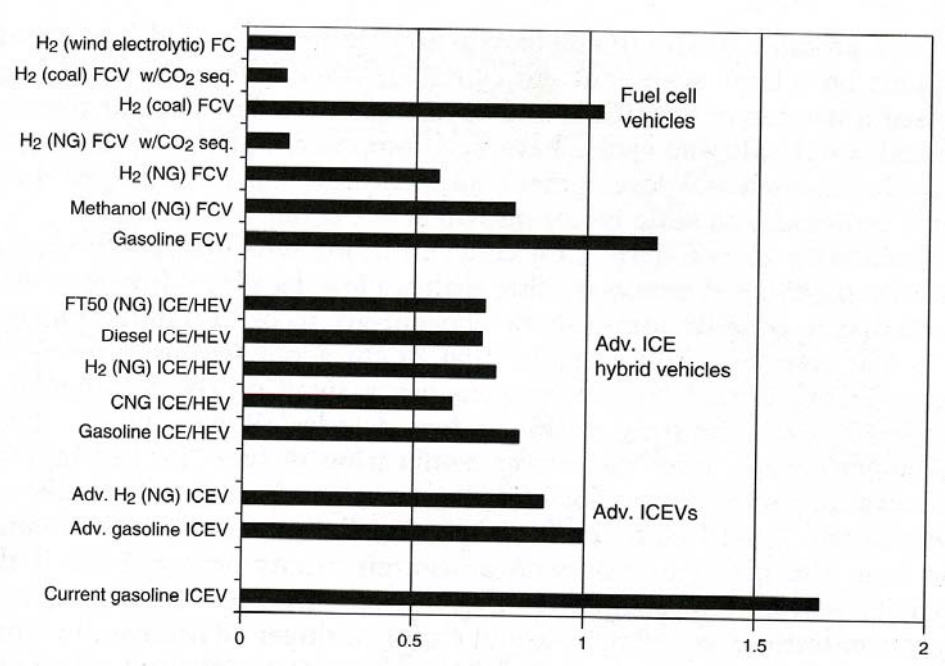

Figure 2. Well to wheels GHG emissions normalized to efficient gasoline vehicles.[7-12]

Hydrogen produced from coal is anticipated to be the main option for near- and mid-term solutions because there are large reserves in the United States as well as the rest of the world. Currently 18% of the world's hydrogen is made from coal.[13] Although producing hydrogen from coal is more capital intensive then production from natural gas,

the costs of coal are less than that of natural gas.[6] The United States Department of Energy's Office of Fossil Energy has been continuously soliciting industrial interest in the FutureGen plant, a coal fed plant that will produce both hydrogen and power with reduced CO_2 emission.[14,15]

In summary, steam reforming is currently the benchmark technology of hydrogen production with industrial maturity. Natural gas, coal, and other petroleum products are common feed stocks for catalytic reforming to hydrogen. However, because of the limited resources of these fossil fuels and their associated net CO_2 production, finding renewable sources for hydrogen generation is strategically important to the world's energy security and environmental safety.

Hydrogen from Water Electrolysis

It has been proposed to use different energy sources to produce hydrogen from water via electrolysis, which is free of CO_2 byproduct:

$$2H_2O \xrightarrow[electricity]{} 2H_2 + O_2$$

Electrolysis technology has been used commercially in the gas industry.[16] The proton exchange membrane (PEM) has been used for decades to produce oxygen in submarines and spacecraft, and to produce hydrogen.[17] Because of energy loss due to the limited efficiency in this process, it may not seem beneficial energy-wise to have a fuel cell membrane running in reverse to create hydrogen for a fuel cell. Since neither process is 100% efficient, there would be a net energy loss by the total process. This is not the case when the electricity supplied for electrolysis comes from a cheap or "free" renewable energy source, such as solar and wind energies. Another benefit of this method is that the hydrogen could be produced onsite. This would eliminate the need for hydrogen storage and transportation, which are both fairly expensive and lacking of safety assurance at

present. The major drawbacks to this method are high cost (using electricity from solar and wind energies) and low efficiency.[17]

Hydrogen from Biomass and Other Renewable Resources

Production of hydrogen and liquid fuels from biomass and organic wastes is considered an effective approach to mitigating the environmental problems caused by pollutant emissions from fossil fuel combustion and allaying our dependence on the limited oil reserves. However, current technological inefficiencies render such biomass utilization economically unviable. Technologies for production of hydrogen from biomass or by bioprocess including high-temperature pyrolysis combined with catalytic reforming processes[18,19] and direct photocatalytic and biosynthesis[20] have been explored in recent years. These strategies, however, encountered problems of low catalyst efficiency and very limited productivity.

An alternative to realizing the goal of "hydrogen from biomass" is to produce intermediate carbohydrates or hydrocarbons from biomass via bioprocesses or biochemical processes and then convert the intermediates to H_2 through subsequent chemical processes. For example, CH_4 can be produced from biomass by cost-effective technologies such as anaerobic fermentation while the existing natural gas infrastructure can be used for storage, transportation, and processing of the vast volume of CH_4 products. However, conversion of CH_4 to H_2 and CO_2 also lacks technologies that can meet the economic targets proposed by the DOE (i.e. $3.00 per gallon equivalent). Technologies currently under investigation for CH_4 conversion include the syngas and water-gas shift (WGS) processes, high-temperature catalytic pyrolysis[21-23] and low-temperature, two-step nonoxidative dehydrogenation[24,25].

Hydrogen production from municipal wastes is also being researched.[26,27] Pretreatment of the waste creates a slurry of suitable viscosity and heating value for efficient production of hydrogen. The key component in this process is the downdraft gasifier, which has four reaction zones: drying, pyrolysis, oxidation and reduction zones. Sewage sludge is a renewable resource that can successfully produce hydrogen; however, the downsides are low production rates and high cost.

The exothermic WGS process converts all the carbon to CO_2 and CO, which requires costly processes to purify and sequestrate in order to produce H_2 without significant emission of greenhouse gases to the atmosphere. Nonoxidative pyrolysis is an endothermic process, which does not generate CO_2. The pyrolysis reaction, however, must be operated at extremely high temperatures (typically above 1250°C), requiring expensive, thermally resistant equipment and high-grade heat. A large amount of nonreactive graphite carbon is usually generated that can deactivate the catalyst or insulate the heating elements. The nonoxidative dehydrogenation method mainly produces higher hydrocarbons with H_2 as "hydrogen byproduct" and is also limited by its low conversion and two-step barrier.

Microalgae has also been shown to successfully reform hydrogen from biomass at temperatures ranging from 850-1000^{o}C.[28,29] This method is based on catalytic steam gasification of biomass with concurrent separation of hydrogen in a membrane reactor. The membrane reactor is selective to hydrogen and separates it as it is produced. Again one of the major problems with hydrogen from algae is the low production rate of hydrogen.

More recently, the method of catalytic conversion of biomass-derived carbohydrates to hydrogen has shown great potential for production of renewable hydrogen. The reaction is carried out at the surface of metal catalyst, e.g. Pt, Pd, Co, Rh and Ru, in liquid water under elevated temperature and high pressure.[18,30,31] However, other catalysts such as Sn and Ni have successfully been used to reform hydrogen.[32,33] Using liquid phase reforming of oxygenated hydrocarbons eliminates the need to vaporize water and the oxygenated hydrocarbon, thereby reducing the energy requirements.[17] The current operating temperature for this reaction is less than 300^{o}C under pressures slightly above the autogenous vapor pressure of the feed solution.

Experiments have been run using γ-Al_2O_3-supported platinum catalysts (3wt%Pt load) by Cortright et. al.[18,34] Their experimental results on different oxygenated hydrocarbon molecules are shown in Table 1 and Figure 3. The H_2 selectivity decreases as the number of carbons in the oxygenated hydrocarbon molecule increases.

Table 1. Experimental results for reforming of oxygenated hydrocarbons to hydrogen at 498 K and 538 K.[18]

	Glucose		Sorbitol		Glycerol		Ethylene Glycol		Methanol	
Temperature (K)	498	538	498	538	498	538	498	538	498	538
Pressure (bar)	29	56	29	56	29	56	29	56	29	56
% Carbon in liquid effluent	51	15	39	12	17	2.8	11	2.9	6.5	6.4
% Carbon in gas-phase effluent	43	84	61	90	83	99	90	99	94	94
Gas-phase compositions										
H_2 (mol %)	51	46	61	54	65	57	70	67	75	75
CO_2 (mol %)	43	42	35	36	30	32	29	29	25	25
CH_4 (mol %)	4	7	2.5	6	4.2	8.3	0.8	2	0.4	0.6
C_2H_6 (mol %)	2	2.7	0.7	2.3	0.9	2	0.1	0.3	0	0
C_3H_8 (mol %)	0	1	0.8	1	0.4	0.7	0	0	0	0
C_4, C_5, C_6 alkanes (mol %)	0	1.2	0	0.6	0	0	0	0	0	0
% H_2 Selectivity	50	36	66	45	75	51	96	88	99	99
% Alkane Selectivity	14	35	15	32	19	31	4	8	1.7	2.7

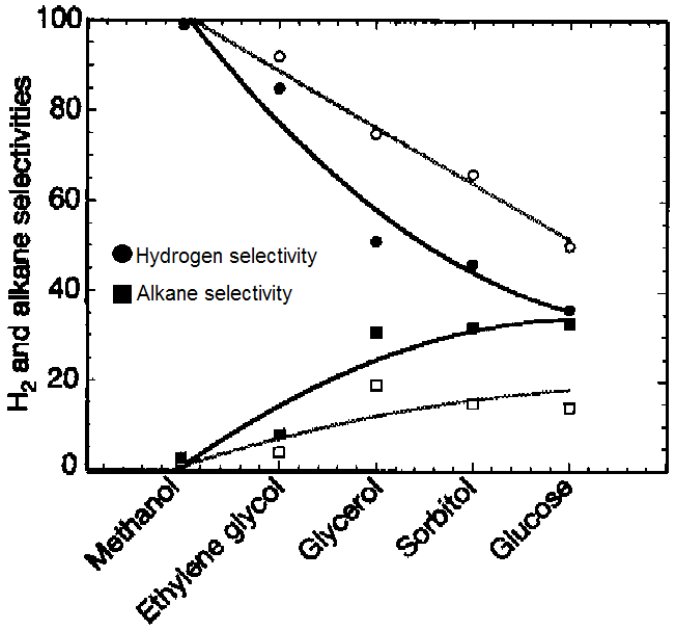

Figure 3. Selectivity of hydrogen and alkanes.[18]

Figure 4 below shows a schematic representation of the reaction pathways believed to be involved in the formation of H_2 and alkanes over a platinum catalyst (Pt).

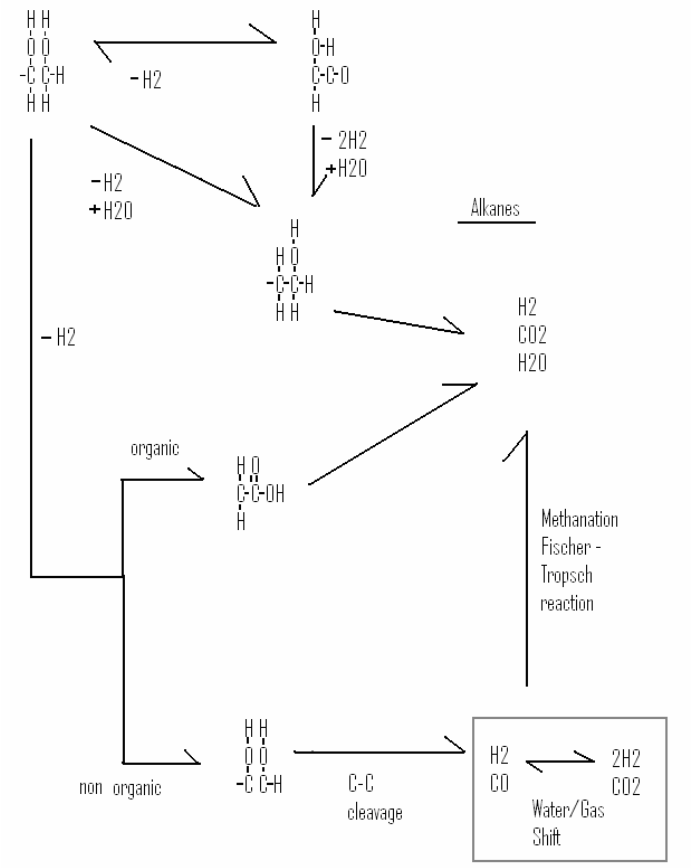

Figure 4. Proposed reaction pathways for production of H_2 by reaction of oxygenated compounds and water.[18]

The first step for the reactant (carbohydrate) is to undergo a dehydrogenation step on the metal surface to create adsorbed intermediates before the C-C or C-O bonds are cleaved.[18] The cleavage activation barriers for O-H and C-H bonds is similar, but Pt-C bonds are more stable than Pt-O bonds. Thus, the reactant is most likely bonded to the surface via the Pt-C bond. As seen on the bottom reaction pathway, cleavage of the C-C bond will then lead to the formation of CO and H_2. CO will then react with water to form CO_2 and H_2 via the water-gas shift reaction. The further reaction of CO_2 with H_2 will then form alkanes and water by methanation and Fischer-Tropsch reactions:[30]

$$CO_2(g) + H_2(g) \leftrightarrow CH_4(g) + 2H_2O(g)$$

The reactant needs to remain on the catalyst surface long enough to form CO_2 and H_2, but these two products must immediately leave the surface before they react to form alkanes and water. Undesirable alkanes can also be formed from the other two reaction pathways after dehydrogenation by the cleavage of the C-O bond. This process presents a parallel selectivity challenge. Another parallel reaction selectivity challenge occurs from cleavage of C-O bonds via dehydration reactions catalyzed by acid sites associated with the catalyst support, or catalyzed by protons in the aqueous solution followed by hydrogenation reactions on the catalyst.[18]

Although the proof-of-concept was successful, the commercial realization of H_2 production from renewable biomass through this catalytic reforming process demands new catalysts that can provide higher conversion rates and H_2 selectivity and a capability to work with feed streams of higher concentration (higher throughput), while the cost of catalyst must also be reduced.

OBJECTIVE AND TASKS

The main objective of this proposed research is to develop new Pt/NaY zeolite catalysts for high-efficiency liquid (water)-phase conversion of biomass-derived carbohydrates to H_2. The specific tasks of this research include:

1. To design and establish a packed-bed reactor system for high pressure liquid phase reaction. The reactor system will be tested by using a similar catalyst (i.e. Pt/γ-alumina) to that reported in the literature.
2. To synthesize and characterize Pt/NaY and Pt/γ-alumina catalysts. Synthesis procedures will be developed and optimized for both Pt/NaY and Pt/γ-alumina catalysts. X-ray diffraction (XRD) will be used to confirm the structure of both catalysts. Microprobe analysis will be employed to determine the composition of both catalysts. Scanning transmission electron microscopy (STEM) will be used to determine the Pt cluster size in the Pt/γ-alumina catalyst. Scanning electron microscopy (SEM) will be used to determine the size and morphology of the catalyst particles. Brunauer-Emmett-Teller (BET) N_2 adsorption and desorption will be used to measure the catalyst surface areas. Carbon monoxide (CO)-chemisorption will be measured to determine the Pt dispersion.
3. To select catalysts for catalytic performance evaluation. Catalyst selection will be done based on methanol conversion for Pt/γ-alumina and Pt/NaY catalysts with different Pt load levels. The reaction tests will be conducted at 493 K and 533 K, respectively.

4. To evaluate catalytic performance and stability of the selected catalysts for extended periods of operation time (total continuous reaction time over two hundred hours).
5. To test the selected Pt/NaY catalyst for conversion of both ethanol and glucose in liquid phases.

SYNTHESIS OF CATALYSTS

Platinum and other group VIII metals have been shown to successfully reform hydrogen from a number of oxygenated hydrocarbons because of the group's ability to cleave the C-C bond. Research by R.D. Cortright et. al.[1,30,32-34] has indicated that γ–Al_2O_3 was a suitable support to use for these group VIII metals. However, the productivity by the Pt/γ-alumina catalysts was not high enough for practical considerations. On the other hand, it has been reported in the literature that transition metals loaded in Y-type zeolites exhibit higher catalytic performance for non-oxidative conversion of methane to higher hydrocarbons and H_2 because of the increased reducibility of metal ions in NaY and the metal-zeolite and metal-metal synergistic effects on catalytic properties.[35] In this study, research will be focused on exploring the Pt/NaY catalysts for the liquid phase reforming of carbohydrates to H_2.

Synthesis of Pt/γ-Al_2O_3 Catalysts

The Pt/γ-Al_2O_3 catalysts were prepared by the following procedure:

I. γ-Al_2O_3 nano-particles preparation by sol-gel process;[36]
II. Pt/γ-Al_2O_3 catalyst preparation by incipient wetness impregnation followed by thermal treatments and reduction;
III. Characterization of catalyst particles.

Synthesis of γ-Al_2O_3 Nanoparticles

The sol-gel method was used for the synthesis of γ-Al_2O_3 gel/nanopowders. The synthesis procedure is shown in Figure 5.

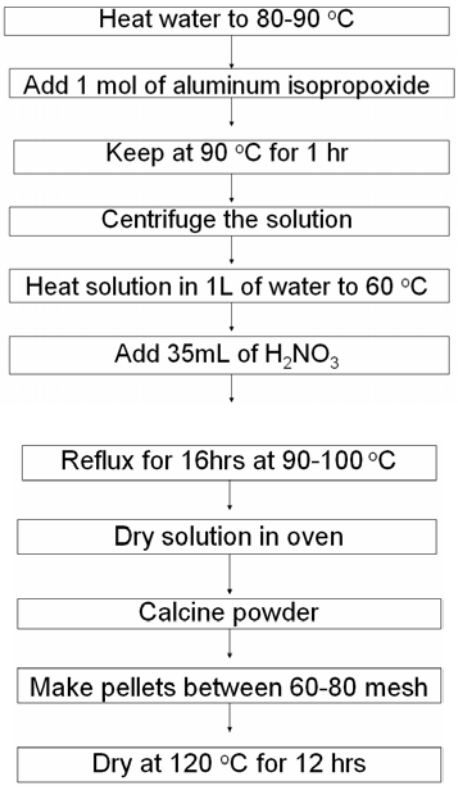

Figure 5. Procedure for preparation of γ-Al_2O_3 nanopowders.

In a 1-Liter three pronged flask, 900mL of water was added. A stir bar was placed into the flask and the flask placed on a magnetic hot plate. The water was then heated to between 80-90^{o}C while being stirred. One mole of aluminum isopropoxide (98+% Sigma-Aldrich) was weighed and added drop-wise to the water once the desired temperature was reached. After all of the aluminum isopropoxide was added, the solution was stirred for one hour. The solution was then centrifuged four times to clean it, and then the recovered gel was re-dispersed in the flask with approximately one liter of water. The resultant suspension was heated to 60^{o}C where 35 milliliters of (1M) HNO_3 was added to form a stable sol. The sol was refluxed for 16 hours at a temperature of 90-100^{o}C in the flask with two of the prongs plugged and the third mounted with a reflux column. After reflux was completed, the sol was placed in an oven at 80^{o}C and dried for

approximately four days to obtain a dry gel. The dry gel was then calcined in air in a furnace (CM Inc. High Temp Furnace) by the following program:

(i) Heat up from 50°C to 450°C at a rate of 1°C/min;

(ii) Hold at 450°C for 3 hours;

(iii) Cool down from 450°C to 50°C at a rate of 1°C/min.

The calcined γ-Al_2O_3 pellets were then ground to 60-80 mesh size and further dried in an oven at 120°C for 12 hours.

Pt-loading by Impregnation

The platinum was loaded by impregnation using a tetraamine platinum (II) nitrate {$[Pt(NH_3)_4]$ $(NO_3)_2$} precursor solution (99%; Sigma-Aldrich). The basic steps for the incipient wetness impregnation process are given below in Figure 6:

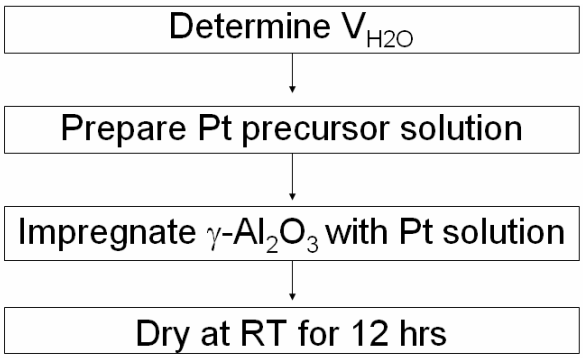

Figure 6. Procedure for incipient wetness impregnation.

First, the amount of water (V_{H2O}) required for completely wetting the amount of γ-Al_2O_3 catalyst to be prepared was determined. For example, if 4 grams of catalyst were to be made, 4 grams of γ-Al_2O_3 dry powder was weighed and place in a small beaker. Water was then added drop-wise until all of the γ-Al_2O_3 was saturated and the volume of water (V_{H2O}) used was recorded. For a desired weight percentage of Pt load, the amount

of {[$Pt(NH_3)_4$] ($NO_3)_2$} needed was thoroughly mixed with V_{H2O} of water. The γ-Al_2O_3 powder was then impregnated with this precursor solution. The wet γ-Al_2O_3 gel was then dried at room temperature for 12 hr and stored in a sealed sample bottle before use.

Calcination

One gram of catalyst was put into a stainless steel tube (4" long and diameter of ⅛"). The tube was then mounted into gas flow system in a furnace. The catalyst was then calcined using the following procedure:

(i) A mixture of oxygen (10 vol.% O_2) and helium (90 vol.% He) was passed through the reactor at a total flow rate of 40 mL/min;

(ii) The furnace was heated from 50^{o}C to 260^{o}C at a rate of 1^{o}C/min;

(iii) The furnace was held at 260^{o}C for 2 hours;

(iv) The temperature was then cooled from 260^{o}C to 50^{o}C at a ramp rate of 1^{o}C/min.

Catalyst Reduction

The catalyst was reduced in hydrogen using the following procedure:

(i) Pure hydrogen was passed through the catalyst powders (in SS tube) at a rate of 25 mL/min;

(ii) The furnace was heated from 50^{o}C to 260^{o}C at a heating rate of 1^{o}C/min;

(iii) The furnace was held at 260^{o}C for 2 hours under hydrogen flow;

(iv) The temperature was cooled from 260^{o}C to 50^{o}C at a ramp rate of 1^{o}C/min.

Synthesis of Pt/NaY Catalysts

The Y type zeolite has a high surface area with a uniform pore size of ~0.74 nm making it desirable for applications as catalysts and catalyst supports. Transition metal-loaded NaY zeolite catalysts have been previously demonstrated in our group to be highly active to catalyze methane dehydrogenation.[25] In this work, NaY zeolite crystals

were synthesized by hydrothermal crystallization and the platinum was loaded into the zeolite pores by ion exchange followed by thermal treatments and H_2 reduction process. The following procedure was used to fabricate Pt/NaY particulate catalyst.

(i) Hydrothermal synthesis of NaY particles;

(ii) Ion exchange to load $[Pt(NH_3)_4]^{2+}$;

(iii) Calcination;

(iv) Catalyst reduction.

Zeolite Particle Synthesis

The procedure for synthesis of the NaY zeolite particles is shown in Figure 7. First, sodium hydroxide (99.998% Sigma-aldrich), sodium aluminate anhydrous (Riedel-deHäen), and water were mixed together in a 250 milliliter flask. The mixture was stirred vigorously for 30 minutes. Water glass (~14%NaOH and 27%SiO_2 Sigma-aldrich) was then added followed by another 12 hr of strong stirring. The overall molar composition of the synthesis gel was $Al_2O_3 : 12.8SiO_2 : 17Na_2O : 675H_2O$.[37] Once the solution was thoroughly mixed, it was heated for 12 hours at 363 K in an autoclave for hydrothermal crystallization. After the hydrothermal treatment, the powders were recovered from the autoclave and washed with DI water to a pH of ~7 by centrifuging.

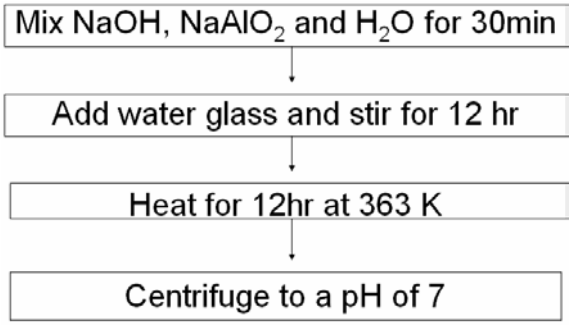

Figure 7. Procedure for making NaY zeolite.

Pt loading by Ion Exchange

Ion exchange was performed by the procedure outlined in Figure 8. First, the Pt precursor $[Pt(NH_3)](NO_3)_2$ was dissolved in water and mixed with the NaY zeolite powder in a small beaker. The beaker was then placed into a water bath at 363 K for one hour. The ion-exchanged Y-zeolite was centrifuged and rinsed by DI water until a pH of 7.5 was obtained. The particles were then dried at 323 K for 12 hours.

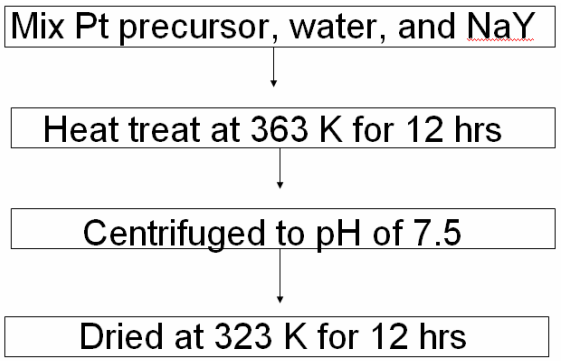

Figure 8. Procedure for Pt-loading via ion exchange.

Ion exchange was conducted for multiple times to increase the amount of platinum exchanged. For the zeolite catalysts made in this work, ion exchange was performed one to three times to vary the amount of platinum loaded into the zeolite.

Calcination

One gram of catalyst was put into a stainless steel U-tube (3" long on each side of the U and ⅛" in diameter). The tube was then connected to the gas flow system in a furnace. The catalyst was then calcined using the following procedure:

(i) A mixture of oxygen (10 vol.% O_2) and helium (90 vol.% He) was passed through the reactor with a total flow rate of 40 mL/min;

(ii) The furnace was heated from 50^{o}C to 260^{o}C at a heating rate of 1^{o}C/min.

(iii) The furnace was held at 260^{o}C for 2 hours;

(iv) The temperature was then cooled from 260^{o}C to 50^{o}C at a ramp rate of 1^{o}C/min.

Catalyst Reduction

The catalyst was reduced in a hydrogen flow using the following procedure:

(i) Pure hydrogen was passed through the catalyst at a rate of 25 mL/min;

(ii) The furnace was heated from 50^{o}C to 260^{o}C under hydrogen flow at a heating rate of 1^{o}C/min.

(iii) The furnace was held at 260^{o}C for 2 hours;

(iv) The temperature was cooled from 260^{o}C to 50^{o}C at a ramp rate of 1^{o}C/min.

CHARACTERIZATION OF CATALYSTS

The catalysts were characterized using XRD and microprobe analysis to confirm the catalyst structure and chemical composition. STEM and SEM were used to determine Pt cluster size and the size and morphology of the catalyst particles, respectively. The catalyst surface area and Pt dispersion were determined by BET using N_2 sorption/desorption, and CO-chemisorption measurements, respectively.

XRD Examination

X-ray diffraction (XRD D/Max $K_{Cu\alpha}$) was used to confirm the phase purity of γ-Al_2O_3 and the presence of platinum presence in the Pt/γ-Al_2O_3. Figure 9 shows the XRD patterns of γ-Al_2O_3, PtO/γ-Al_2O_3, and Pt/γ-Al_2O_3 samples. All three patterns had the characteristic peaks of γ-Al_2O_3. Neither the PtO nor Pt were distinguishable in the XRD patterns likely because of the extremely small size of the PtO or Pt clusters, which were evenly distributed over the γ-Al_2O_3 surface as indicated by the TEM images later.

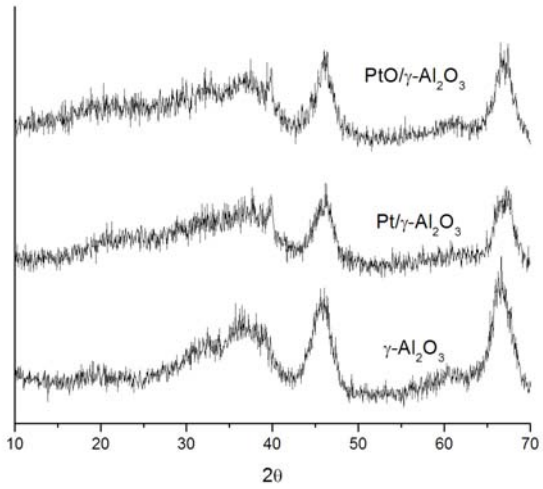

Figure 9. XRD patterns of γ-Al_2O_3 and Pt-loaded γ-Al_2O_3 powders.

XRD was also used to confirm the zeolite structure. The XRD patterns showed that zeolite crystals are pure Y-type without appreciable impurity phases. Again, the characteristic peaks of Pt metal were not seen in the pattern of the Pt-loaded NaY (wt%) samples because Pt was highly dispersed in the zeolite pores.

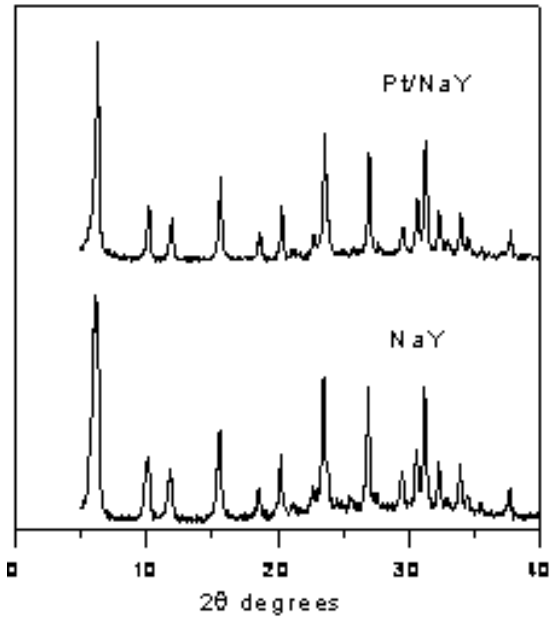

Figure 10. XRD pattern of NaY zeolite and Pt/NaY.

Microprobe Analysis

Microprobe analysis (Cameca SX100) was conducted to quantitatively determine the amount of Pt in the Pt/γ-Al_2O_3 and Pt/NaY catalysts. The results for three catalysts with different loads are listed in Table 2. Microprobe analysis also verified that the silicon to aluminum atomic (Si/Al) ratio of the synthesized Y-type zeolite was approximately 1.5.

Table 2. Results of microprobe analysis for the Pt/γ-Al_2O_3 and Pt/NaY catalysts.

Catalyst		Pt wt.%
γ-Al_2O_3-supported Pt catalysts	3%Pt/γ-Al_2O_3	2.90
	1%Pt/γ-Al_2O_3	1.10
	½%Pt/γ-Al_2O_3	0.50
Pt-loaded NaY zeolite catalysts	0.25%Pt/NaY (single time ion exchange)	0.25
	0.4%Pt/NaY (two-time ion exchange)	0.40
	0.5%Pt/NaY (three-time ion exchange)	0.50

Microscopic Examinations

STEM (EOL 2010F FASTEM) was used to observe the average size and dispersion state of Pt particles on γ-Al_2O_3. Figure 11a shows that the platinum was evenly distributed on the surface of the γ-Al_2O_3 powders. Figure 11b shows that the Pt particle size was 1~2 nm. Because of the small cluster sizes, high dispersion state, and low load level, the Pt was not shown in the XRD patterns.

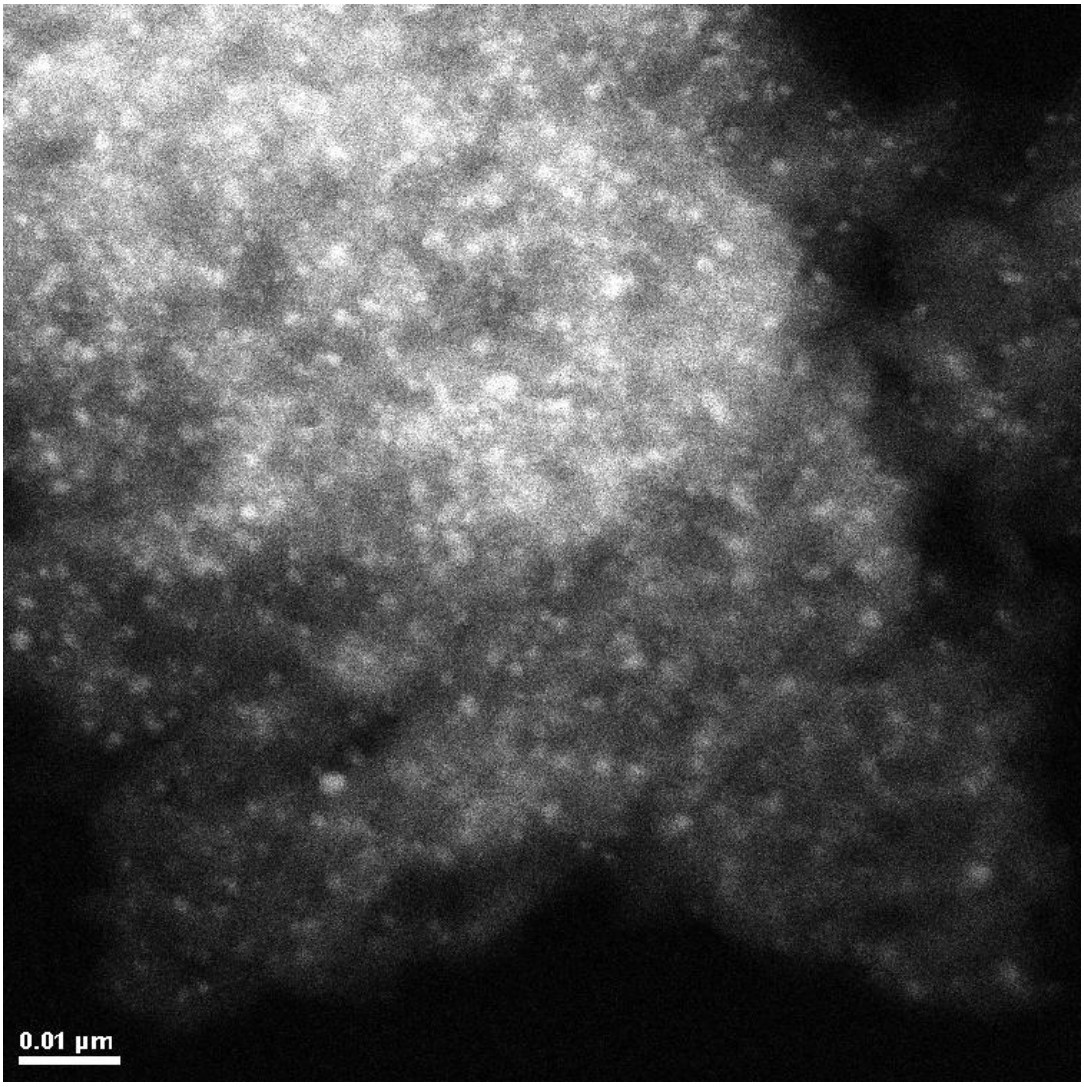

(a)

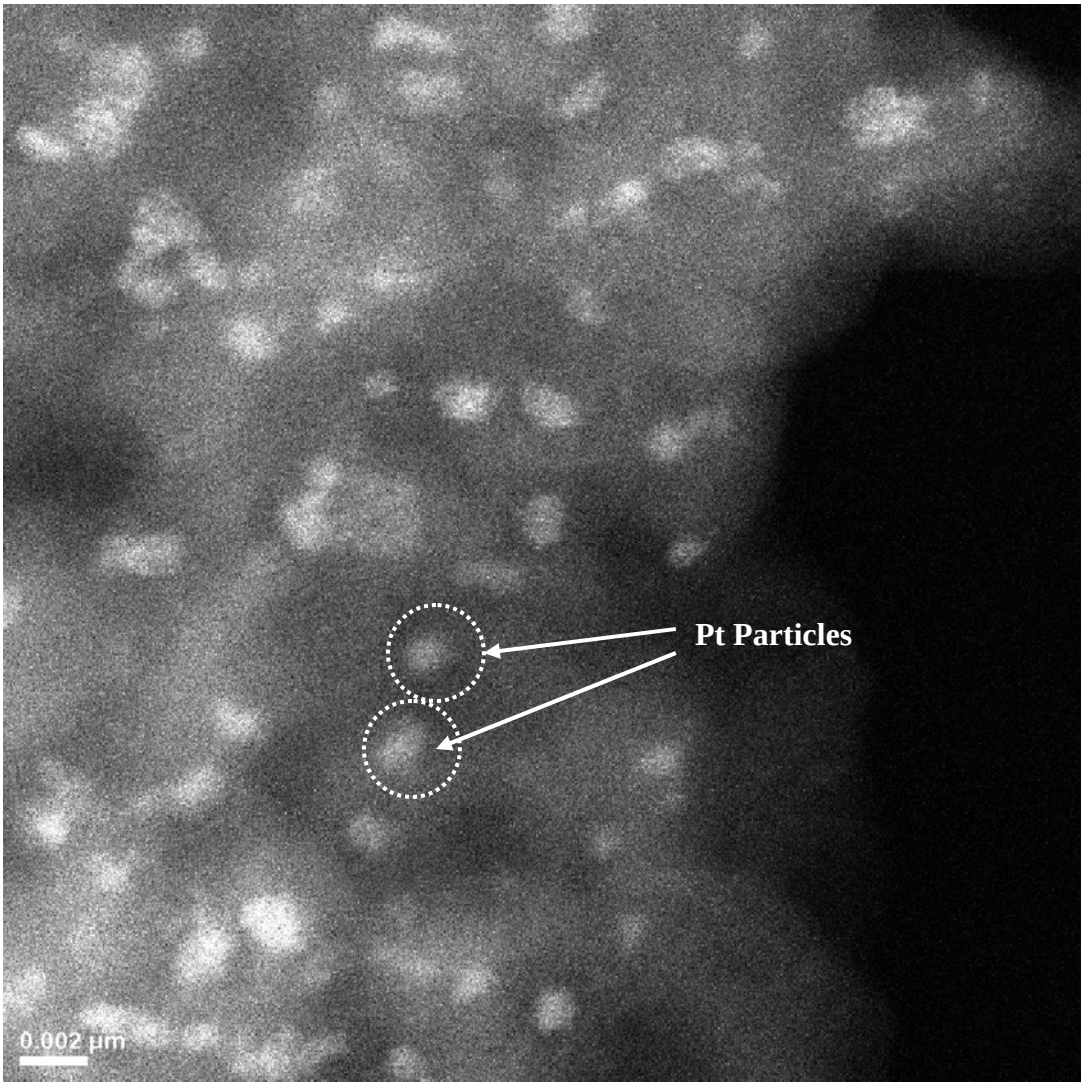

(b)

Figure 11a & b. **STEM images of Pt/γ-Al_2O_3**

The SEM image of the as synthesized NaY zeolite particles and the TEM image of the Pt/NaY catalyst particles are presnted in Figure 12. The average size of the as-synthesized zeolite particles is around 1 micron according to the SEM observation (Fig. 12a). It can be observed from the TEM image (Fig. 12b) that the platinum clusters (with an approximate a diameter of 1.2 nm) located in the cages although some zeolite crystals might collapse under the field emission during observation. Energy Dispersive

Spectroscopy (EDS) was also conducted to verify the amount of Pt in the particles. It was found that the concentration of Pt in the center of the zeolite particles was higher than the concentration on the edge of the particles. In some instances, the concentration of Pt in the center of the zeolite particle was twice as much as that on the edge of the zeolite particle. This may be caused by the beam size, which covered part of the void when sampling the edge.

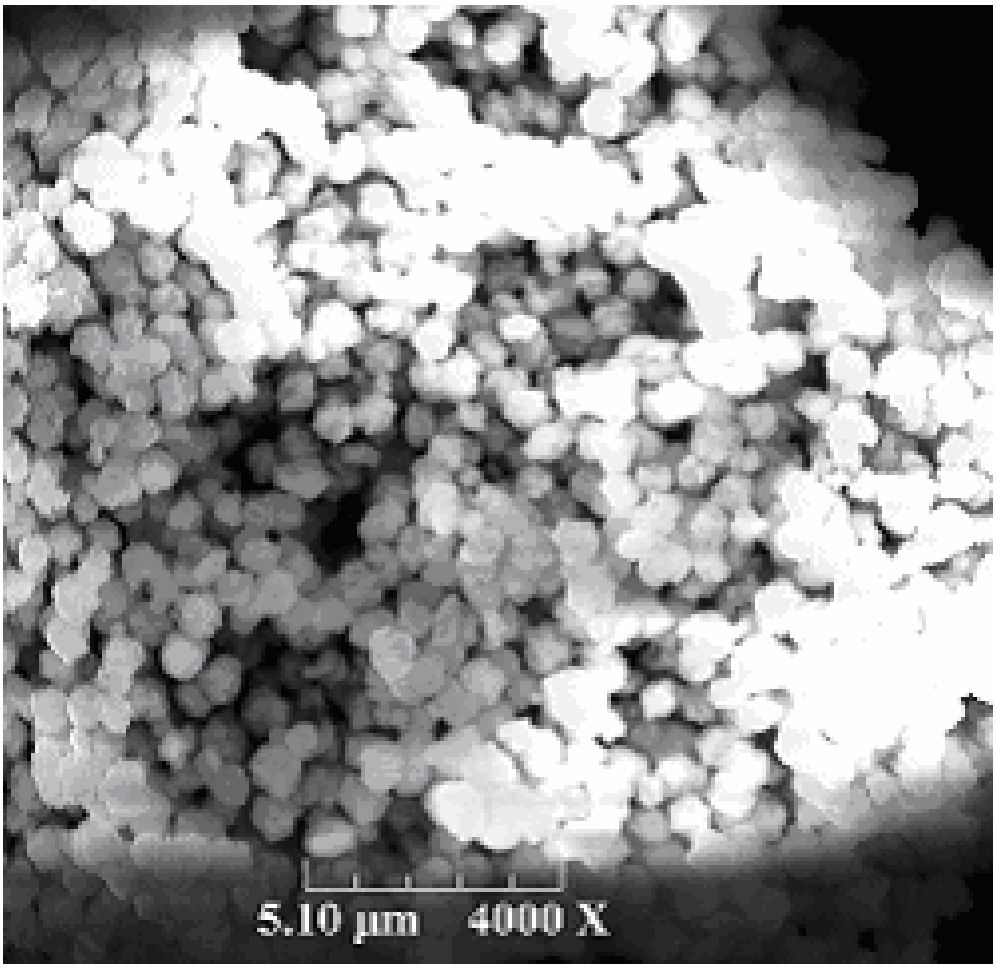

(a)

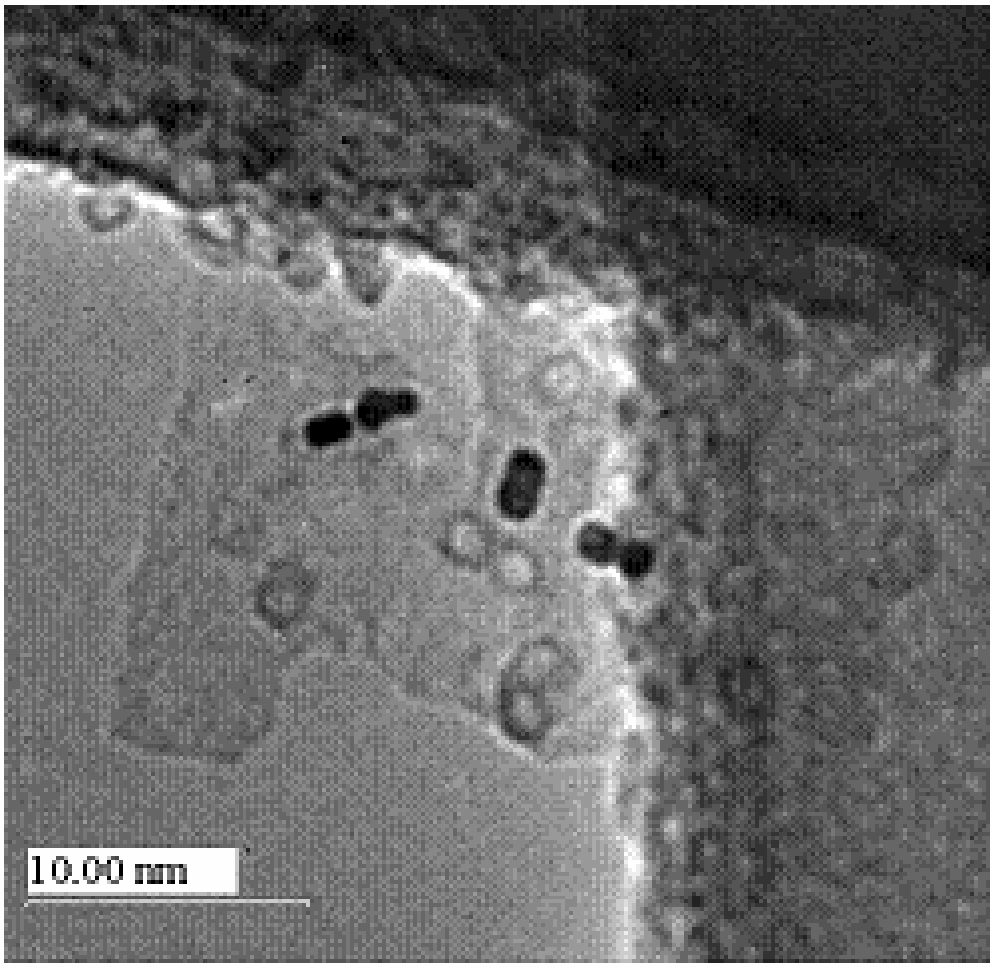

(b)

Figure 12. (a)SEM image of the as-synthesized NaY zeolite particles and (b) TEM image of the Pt/NaY catalyst particles

BET and Chemisorption Testing

The BET technique (ASAP 2020, Micromeritics) was employed to determine the surface area and micropore volume of the Pt/γ-Al_2O_3 and NaY catalysts using N_2 as the probe gas. The results are given in Table 3. Carbon monoxide (CO)-chemisorption (ASAP 2020, Micromeritics) was also performed to determine the Pt dispersion. The metal dispersion values were used to calculate the turnover frequency numbers for the catalysts during the catalytic reforming reaction. It was observed that the Pt dispersion in

the Pt/NaY catalyst decreased with the increasing of the load level. The NaY catalyst also had a much higher area than that of the γ-Al_2O_3 catalyst. It was observed that the Pt dispersion of the Pt/NaY catalyst decreases with increasing the Pt loading level. The Pt dispersion level of the 3%Pt/γ-Al_2O_3 was much lower compared to the Pt/NaY catalysts.

Table 3. Surface areas, micropore volumes, and Pt dispersion of the Pt/γ-Al_2O_3 and Pt/NaY catalysts with different Pt-loading levels.

Support	NaY			γ-Al_2O_3		
BET area	715.4 m^2/g			259.3 m^2/g		
Micropore Volume	0.31 cm^3/g STP			0.36 cm^3/g STP		
	Pt load wt%	CO uptake mmol/g	Dispersion	Pt load wt%	CO uptake μmol/g	Dispersion
	0.25 wt% Pt	8.8	34%	0.5 wt% Pt	-	-
	0.4 wt% Pt	11.8	29%	1.1 wt% Pt	-	-
	0.5 wt% Pt	11.8	23%	2.9 wt% Pt	58.6	17%

EVALUATION OF THE CATALYSTS FOR LIQUID PHASE REFORMING OF METHANOL TO HYDROGEN

Packed-Bed Reactor System

A packed-bed reactor system was established, which consisted mainly of three parts as shown schematically in Figure 13. The first part is the flow control unit, which includes a syringe pump (LC 500, ISCO) for precise high pressure liquid feed, and a high pressure gas system, which provides the sweep gas (N_2). The second part is the reactor consisting of a packed-bed column in a furnace and a high-pressure flash tank for separating the gaseous products from the reactor outlet stream. The third part is an HP 5890 (II) gas chromatograph (GC) equipped with a Thermal Conductivity Detector (TCD) and a Hayesep GC column for separation.

During the reaction test, a 1% solution of methanol (MeOH) was stored in the syringe pump with a capacity of 500 mL. A flow rate of 0.8 mL/hr was used so that a WHSV value of 0.008 (grams of oxygenated compound per gram of catalyst per hour) through the reactor was obtained. This value was chosen so that the data obtained could be compared to the literature results, which were obtained under same operating conditions.[18] One gram of catalyst was placed into the packed-bed column (dimensions given in Calcinations Section) which was mounted in a temperature-programmable furnace (Vulcan 3-550). The catalyst particles were mixed with quartz wool for better distribution and packing effects.

The 1% MeOH solution (feed) was pushed through the packed-bed reactor where it reacted and then entered the gas/liquid separator. The liquid in the flash separator was collected for total organic compound (TOC) analysis **(**Shimadzu TOC-V Carbon Analyzer**)**. The N_2 sweep gas flowed through the gas/liquid flash tank to carry the gas

product for GC analysis. The N_2 gas pressure was kept slightly above the autogenous vapor pressure of the 1 wt.% MeOH solution to ensure a liquid phase in the reactor. A back pressure controller (Cole-Parmer CP-32505-42) was used to control the pressure in the reactor and regulate the pressure of the stream flowing to the GC. The back pressure controller also controlled the carrier gas flow rate to the GC, which was set to 7 (STP) mL/min. A valve was placed between the furnace and the isobaric flash separator to shut of the liquid flow in case of emergency shutdown. Another valve was place at the bottom of the isobaric flash separator for liquid drain at the completion of the experiment. Safety valves were located between the N_2 gas cylinder and the isobaric flash separator and between the isobaric flash separator and the back pressure controller.

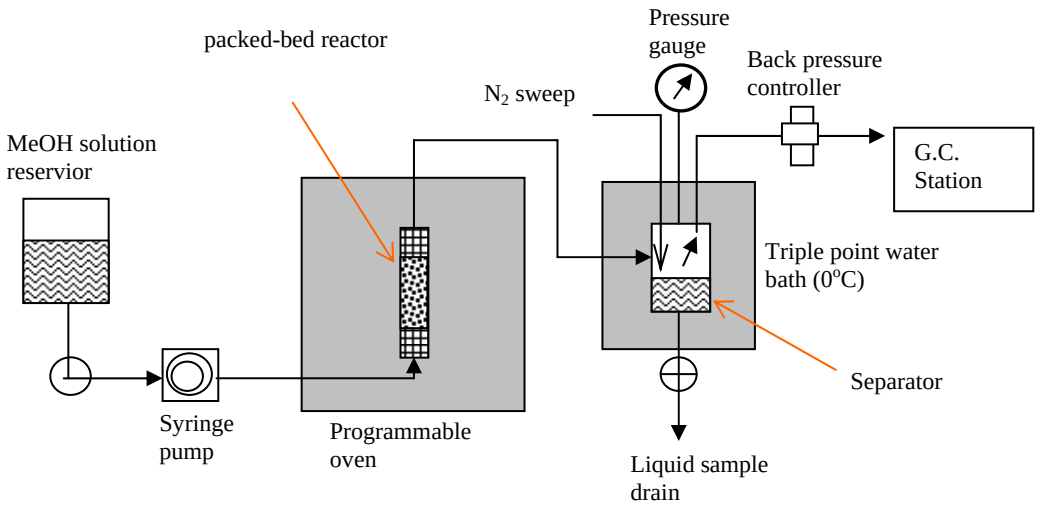

Figure 13. Schematic of reaction system.

Operation Procedure for the Reactor System

The following procedure, as given in Figure 14, was used to activate the catalyst and for testing the catalytic performance of the Pt/γ-Alumina and Pt/NaY catalysts.

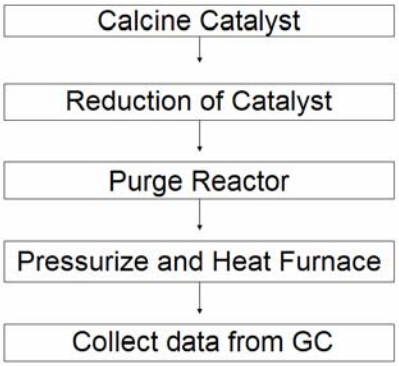

Figure 14. Steps in catalyst preparation and testing of the catalyst.

The catalysts were calcined and reduced according to the procedures previously described. The reactor was then purged with N_2 for two hours at a flow rate of 20 mL/min following the reduction step. Liquid feed solution was then flowed through the reactor to the isobaric flash separator. When the first drop of liquid reached the isobaric flash separator, the valve between the furnace and the isobaric flash separator was closed in order to increase the liquid feed pressure. The system was then slowly pressurized with N_2 (380 psi for a reaction temperature of 220^{o}C, and 760 psi for a reaction temperature of 260^{o}C). After being pressurized, the valve between the furnace and the isobaric flash separator was opened so that the pressure of the reaction system would equilibrate. The gas flow rate to the GC was then set to 7 mL/min and stabilized. After the N_2 (to GC) flow rate was stabilized, the syringe pump was set to pump at a flow rate of 0.8 mL/hr. The furnace was then turned on with the following ramping:

I. Furnace heated at a rate of 3^{o}C/ min from 50^{o}C to 220^{o}C (or 260^{o}C)

II. The furnace was held at the desired temperature for 24 hrs (reaction time).

Figure 15 below shows the process for shutting down the reaction system.

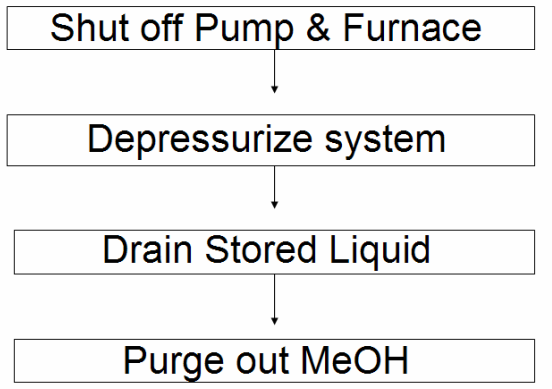

Figure 15. Steps to shutting down the reaction system.

After the test was finished, the temperature was decreased at a rate of 3°C/ min from 220°C (or 260°C) to 50°C. The valve between the furnace and isobaric flash separator was shut. The pump was then turned on and off based upon the liquid feed pressure inside the reactor. This was done in order to make sure that the pressure was higher than that of the autogenious vapor pressure of the feed solution. The N_2 gas that pressurized the rest of the system was slowly bled off until atmospheric pressure was reached. The liquid in the isobaric flash separator was then drained and kept in refrigeration for future TOC analysis. Once the furnace reached room temperature, the valve between the furnace and isobaric flash separator was opened so that N_2 could flow through to sweep out the remaining MeOH solution in the system. The stainless steel tubing was then removed from the furnace and the catalyst was removed and saved.

Results and Discussion

The initial catalyst evaluations were performed for liquid phase reforming of a methanol solution at a temperature of 493 K. The catalysts evaluated include: 3% Pt/γ-Al_2O_3, 1% Pt/γ-Al_2O_3, 0.5% Pt/γ-Al_2O_3, 0.5% Pt/NaY, 0.4% Pt/NaY and 0.25% Pt/NaY.

All of the catalytic reactions were stabilized for over 20 hours and the experimental data were taken after stabilization.

The hydrogen production rate was calculated from carrier gas flow rate and composition of the gas product stream. The selectivity was calculated by the following equation:

$$H_2 \text{ selectivity} = \frac{n_{H2\ producted}}{n_{H2\ produced} + 2n_{CH4\ produced}}$$

Where $n_{H2\ producted}$ and $n_{H2\ producted}$ are the mole flow rates of H_2 and CH_4 in the product stream measured by the GC. The methanol conversion rate is defined as the fraction or percentage of the MeOH in the feed reacted after going through the reactor.

The results are presented below in Figure 16 and Figure 17. Figure 16 shows the hydrogen production rate as a function of the Pt load for the zeolite and γ-alumina supported catalysts and Figure 17 shows the conversion and selectivity of the catalysts versus Pt load.

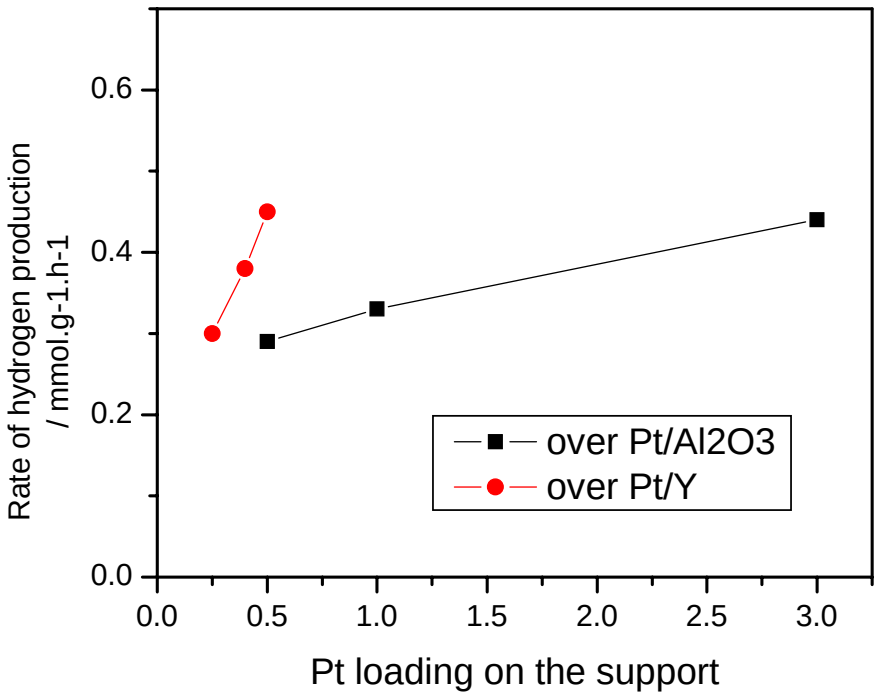

Figure 16. Hydrogen production rate as a function of Pt loading. Solid circles are for Pt/γ-Al_2O_3 catalysts with Pt loads of ½%, 1%, 3 wt%; Solid squares are for Pt/NaY catalysts with Pt loads of 0.25%, 0.4% and 0.5%; reaction conditions: 493 K, 2.6 Mpa, WHSV=0.008 h^{-1}, with 1 wt% methanol solution feed.)

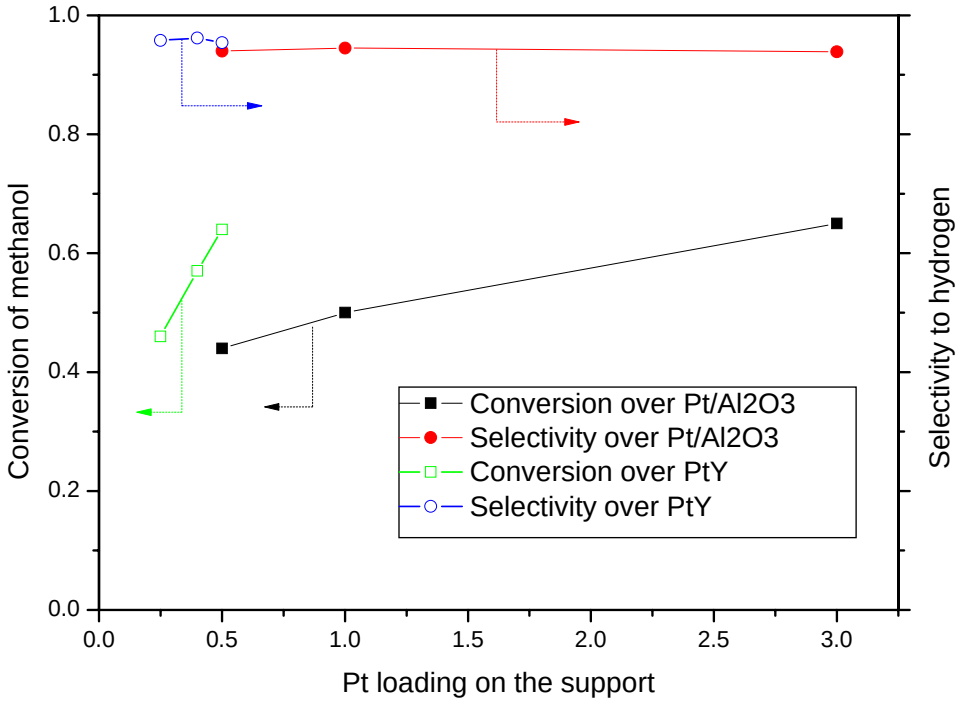

Figure 17. MeOH conversion rate and selectivity as functions of Pt load. Reaction conditions: same as that described in Figure 16.

For both the Pt/γ-Al_2O_3 and Pt/NaY catalysts, the H_2 productivity increased with increasing the Pt load. The 0.5% Pt/NaY had a slightly higher production rate than that of the 3% Pt/ γ-Al_2O_3. The selectivity of all of the catalysts approximately are essentially the same. The methanol conversion increased with an increase in the Pt load for both γ-Al_2O_3 and NaY supported catalysts due to the increased catalyst surface area.

The 3% Pt/γ-Al_2O_3 and 0.5wt% Pt/NaY catalysts, which had the best performance in their respective group, were then further tested for an extended time (>120 hours) to evaluate their stability.

The catalyst stability tests for the 3%Pt/γ-Al_2O_3 and 0.5% Pt/NaY were performed at 498 K and 28.5 bar and 538 K and 55.8 bar, respectively. The results are shown in

Figure 18. Each catalyst was tested at the 498 K first for 120 hrs; then the temperature was increased to 538 K without interruption of the reaction to continue the test for another 120 hrs. Thus, the actual test time was over 240 hrs. No catalyst degradation was observed for either catalyst in the testing period. The 0.5% Pt/NaY catalyst out-performed the 3% Pt/ γ-Al_2O_3 at both temperatures with higher hydrogen productivity.

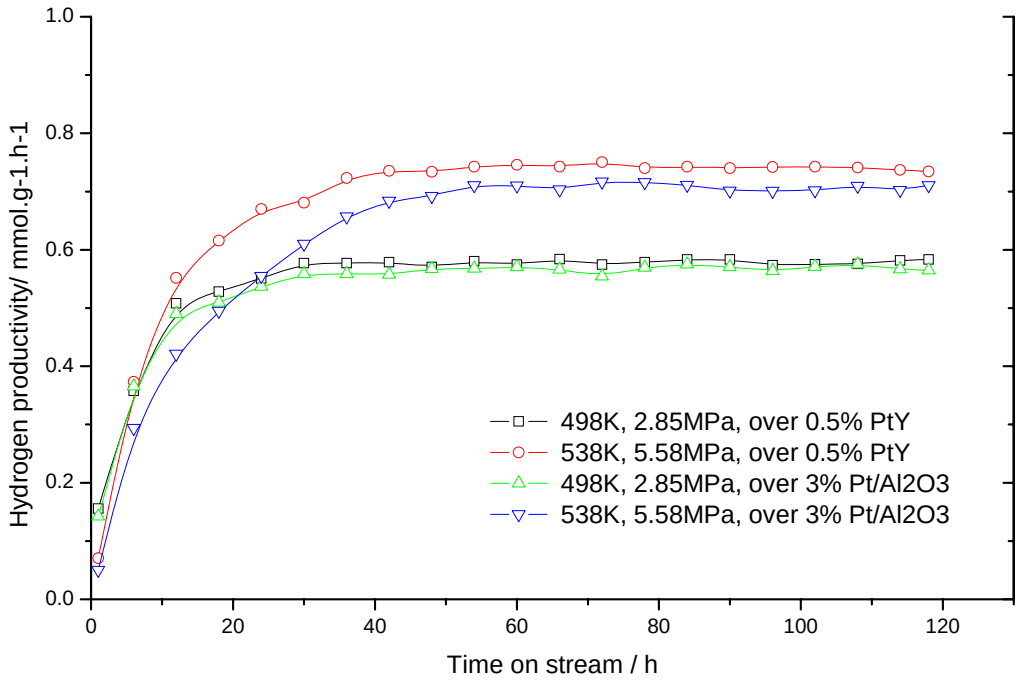

Figure 18. Hydrogen productivity as a function of operation time for liquid phase reforming of methanol over the 3% Pt/γ- Al_2O_3 and 0.5%Pt/NaY catalysts at different temperatures and pressures. Feed conditions: WHSV=0.008 h^{-1} with 1 wt% methanol solution.

Figure 19 below shows the methanol conversion rate and hydrogen selectivity as functions of reaction time. The two catalysts had very similar hydrogen selectivities but the 0.5%Pt/NaY had a higher MeOH conversion rate compared to the 3% γ-Al_2O_3.

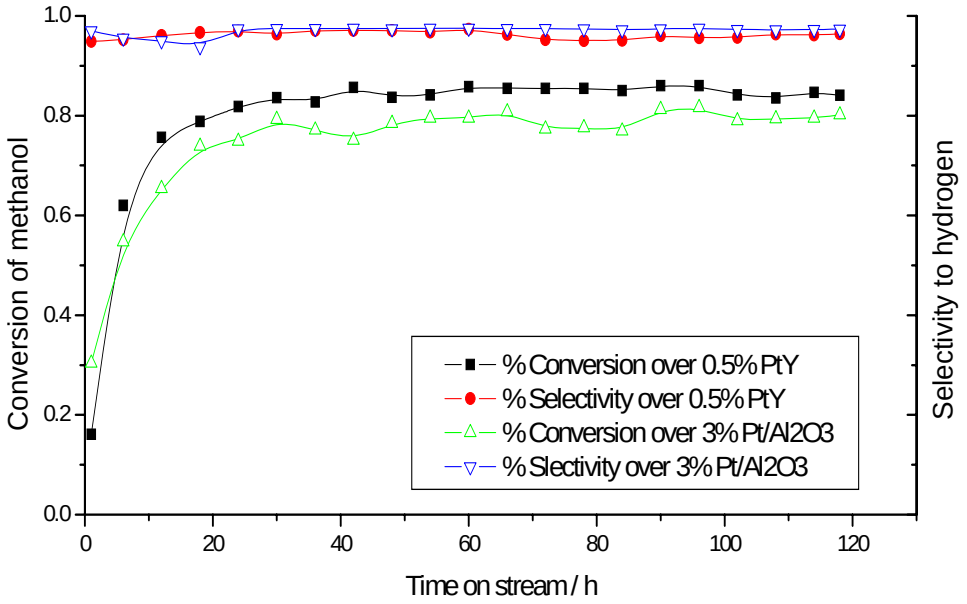

Figure 19. Stability test with 3% Pt/γ- Al_2O_3 and 0.5% Pt/NaY catalysts.

(Reaction conditions: 498 K, 2.9 Mpa, WHSV=0.008 h^{-1}, with 1 wt% methanol solution).

The experimental results of liquid phase reforming of methanol over the two catalysts, namely 3% Pt/γ-Al_2O_3 and 0.5% Pt/NaY, are also shown in Table 4 in comparison with the literature data. The conversion of methanol over the 3%Pt/ γ-Al_2O_3 catalyst at 498 K is lower than that reported in the literature on the same kind of catalysts because the γ-Al_2O_3 support of this work had a much lower surface area than that of the literature γ-Al_2O_3 nanofibers. The Methanol conversion over the 0.5% Pt/NaY catalyst increased with increasing the temperature.

The turnover frequencies (TOF) were calculated from the rates of hydrogen production and then normalized by the number of surface chemisorption sites as determined from irreversible uptake of CO at 308K (or the dispersion values). As shown

in Table 4, the TOF of 0.5% Pt/NaY catalyst is approximately 6 times higher than that of the 3% Pt/γ-Al_2O_3 catalyst and is also much higher than that of the literature.

The catalytic performance of the 0.5% Pt/NaY catalyst is better than that of 3%Pt/γ-Al_2O_3 methanol reforming under the investigated reaction conditions. The high performance of the zeolite supported catalysts may be attributed to the higher dispersion of the Pt metal as well as the synergistic effects between the Pt metal clusters and the zeolite framework. Moreover, the NaY-supported catalysts use much less Pt metal and the NaY is cheaper to produce than the γ-Al_2O_3 nanopowders and nanofibers. Thus, the Pt/NaY catalysts are anticipated to be cost-effective than the traditional Pt/γ-Al_2O_3 catalysts.

Table 4. Table comparing our best two catalysts to those of R. Cortright et. al[1].

	Reference[18]		3%Pt/Al2O3		3x-PtY	
			120 h	120 h	120 h	120 h
T/K	498	538	498	538	498	538
P/MPa	2.86	5.53	2.81	5.51	2.81	5.51
C in Liquid, %	6.5	6.4	19.5	4.8	18.6	0.8
Conversion, %	94	94	78.9	95.5	81.0	98.8
Gas Product						
H_2 (mol,%)	74.6	74.8	74.6	74.5	74.6	74.4
CO_2 (mol,%)	25.0	24.6	24.9	24.9	24.8	24.8
CH_4 (mol,%)	0.4	0.6	0.5	0.6	0.6	0.8
H_2 Selectivity, %[a]	99	99	97.6	97.1	97.1	95.6
Alk Selectivity, %[b]	1.7	2.7	2.0	2.4	2.4	3.0
Rate of H_2 Production[c] /(mmol.g^{-1}.h^{-1})	0.70	0.70	0.57	0.71	0.58	0.74
Turnover frequency /min^{-1}	0.16	0.16	0.16[d]	0.20[d]	0.82[d]	1.04[d]

[a] Based on H-balance, Selectivity of hydrogen = $H_2/(H_2+4\times CH_4)$. [b] Based on C-balance, selectivity of alkane = $CH_4/(CH_4+CO_2)$. [c] WHSV=0.008g of methanol per gram of catalyst per hour. [d] Normalized by the number of surface metal atoms as determined from irreversible uptake of CO at 308K.

TEST OF THE PT/NaY CATALYSTS FOR ETHANOL AND GLUCOSE REFORMING

Ethanol Reforming

Reforming of ethanol to hydrogen is strategically important because of the potential to use ethanol as an intermediate for "hydrogen-from-coal". Ethanol can also be produced by fermenting sugars, a renewable bio-product. However, liquid phase reforming of ethanol to hydrogen has not been reported in the literature so far. Liquid phase reforming of ethanol over 0.5% Pt/NaY catalyst was explored in this work. Table 3 shows that there is relatively low conversion rate (43.8~45.5%) in the liquid phase reforming of ethanol. However, it is encouraging that the selectivity to hydrogen remained high (>80%) and the hydrogen production rates from ethanol (0.79 $mmol.g^{-1}.h^{-1}$ at 538K, 55.8bar) were even slightly higher that that of methanol (0.74 $mmol.g^{-1}.h^{-1}$ at 538K, 55.8bar). The relatively low conversion of ethanol over the Pt/NaY catalysts was probably caused by the slower diffusion of the ethanol molecules in the Pt-loaded zeolite pores and more energy required for C-C bond cleavage as compared to the small methanol molecules.

Table 5. Experimental data for reforming of ethanol over the 0.5% Pt/NaY catalyst.

T/K	498	518	538
P/MPa	2.81	3.88	5.53
Conversion, %	59.6	65.7	68.3
Gas Product			
H_2 (mol,%)	73.9	74.1	74.1
CO_2 (mol,%)	24.6	24.7	24.7
CH_4 (mol,%)	1.2	1.0	1.0
C_2H_6 (mol,%)	0.3	0.2	0.2
H_2 Selectivity, % [a]	94.0	95.2	94.8
Alk Selectivity, % [b]	5.7	4.6	4.6
Rate of H_2 Production[c] /(mmol.g^{-1}.h^{-1})	0.62	0.70	0.79
Turnover frequency[d] / min^{-1}	0.88	0.99	1.10

[a] Based on H-balance, Selectivity of hydrogen = $H_2/(H_2+4\times CH_4+C_2H_6)$. [b] Based on C-balance, selectivity of alkane = $(CH_4+C_2H_6)/(CH_4+2\times C_2H_6+CO_2)$. [c] WHSV=0.008g of ethanol per gram of catalyst per hour. [d] Normalized by the number of surface metal atoms as determined from irreversible uptake of CO at 308K.

Glucose Reforming

Glucose has been successfully reformed to hydrogen over the Pt/γ-Al_2O_3 catalysts. Table 6 gives some results reported in the literature by R.D. Cortright et. al.[1] However, it was found that the hydrogen selectivity in reforming of glucose was much lower than that of in methanol reforming because the hydrogen selectivity in general decreases with a decrease in H/C ratio of the carbohydrate molecule.

Table 6. Data of glucose reforming from literature.[18]

Temperature (K)	498	538
P/MPa	2.86	5.53
% H2 Selectivity	50	36
% Alkane Selectivity	14	35

Liquid phase reforming of glucose over 0.5% Pt/NaY catalyst was also tested at the same reaction conditions as used for the ethanol conversion. Hydrogen in the product steam was undetectable by the gas chromatography during the reaction. This is most likely because the NaY zeolite pores are not accessible to the ringed glucose molecules in liquid phase since the Pt catalysts have been demonstrated to active for reforming of glucose.[1] When glucose dissolves in water, part of the molecular structure changes gradually into *beta*-D-glucose through a *chain*-D-glucose and ultimately achieving dynamic equilibrium (with 36% of *alpha*, 0.02% of *chain* and 64% of *beta* type).[38] Such ringed-structure molecules in aqueous solution are difficult to enter the zeolite pores (diameter of 0.74 nm) due to the steric constraint of the highly polar molecules.[39] This result also suggests that the Pt metal clusters were encaged into zeolite cavities but not deposited on the external surface of the zeolite crystals.

CONCLUSION

In this work, platinum-loaded NaY (Pt/NaY) catalysts were synthesized, characterized, and evaluated for liquid phase reforming of carbohydrates to hydrogen. The catalytic performance of the Pt/NaY catalysts for conversion of methanol to hydrogen was tested in a temperature range of 220 to 265^{o}C and compared to that of the traditional γ-Al_2O_3–supported catalysts (Pt/γ-Al_2O_3), which were also prepared in this study, and the results reported in the literature on Pt/γ-Al_2O_3 catalysts. The Pt/NaY catalysts, although with low Pt loads (~0.5wt.%Pt), were demonstrated to have higher catalytic performance, in terms of hydrogen production rate, selectivity, and methanol conversion, than the benchmark Pt/γ-Al_2O_3 catalysts with high Pt loads (3wt%Pt). Because of the low cost of the NaY zeolite and the low Pt load, the Pt/NaY is promising to be used as a cost-effective catalyst for conversion of biomass-derived carbohydrates to hydrogen. Following are the main findings/conclusions obtained from this research:

(1) Transition metal-loaded zeolites have been demonstrated through the Pt/NaY as a model system to be highly active catalysts for liquid phase conversion of carbohydrates to hydrogen. The Pt/NaY catalysts exhibit higher catalytic performance than the traditional Pt/γ-Al_2O_3 catalysts because of the higher dispersion of Pt in the zeolite structure and the metal-zeolite synergistic effects on the catalytic reaction.

(2) For both the Pt/NaY and Pt/γ-Al_2O_3 catalysts, increasing the Pt-loading level was found to increase the hydrogen production rate in the investigated ranges (0.25% - 0.5%Pt for Pt/NaY and 0.5% - 3%Pt for Pt/γ-Al_2O_3). This is because of the enlarged catalyst surface area with

increasing the Pt load. It was also observed that raising the reaction temperature (from 220 to 265^{o}C) enhanced the hydrogen productivity because of the overall endothermic nature of the reaction. Although the Pt load and the reaction temperature have not been optimized in this study, the reaction conditions in the liquid phase reforming are quite mild compared to the commonly used high temperature technologies.

(3) The Pt/NaY requies much less Pt metal then does the Pt/γ-Al_2O_3 for same catalytic performance. For example, the 0.5%Pt/NaY outperformed the 3.0% Pt/γ-Al_2O_3 in liquid phase reforming of methanol to hydrogen. Taking into account the low cost of zeolite as compared to the cost of γ-Al_2O_3 nano-materials, the zeolite-based catalysts will be of lower cost than the Pt/γ-Al_2O_3 catalysts or other metal oxide nanomateials (e.g. ZrO_2, TiO_2 etc.) supported catalysts.

(4) The Pt/NaY catalysts were also proven to be active for liquid reforming of ethanol but with lower conversion (~46% at 265^{o}C) rate compared to that in methanol reforming (~99% at 265^{o}C). The hydrogen production rate from ethanol reforming, however, was higher than that from methanol reforming. Therefore, because of the readiness for gas (products) and liquid (feed) separation, the potential of Pt/NaY catalysts for ethanol conversion deserves further investigation.

(5) The Pt/NaY catalysts were found to be incapable of reforming the glucose to hydrogen. Since it has been demonstrated in the literature that the Pt catalyst is active for liquid phase reforming of glucose, the incapability of Pt/NaY for glucose conversion is likely due to the difficulty for the highly

polar ringed glucose to inter the 0.74nm zeolite pores to contact the Pt cluster in the zeolite cages.

(6) The successful demonstration of Pt/NaY catalysts for methanol and ethanol liquid phase reforming opens up a new window for developing highly effective transition metal-loaded zeolite catalysts for liquid phase conversion of biomass derived carbohydrates to hydrogen.

REFERENCES

[1] D. Scott. Back from the Future: to Build Strategies taking us to a Hydrogen Age. The Hydrogen Energy Transition. Elsevier. 2004.

[2] D. Sperling, J. Cannon. Introduction and Overview. The Hydrogen Energy Transition. Elsevier. 2004.

[3] J. Larminie, and A. Dicks. Fuel Cell Systems Explained. John Wiley & Sons. 2000.

[4] U.S. Department of Energy. Hydrogen Fuel Cells, and Infrastructure Technologies Program. Washington, DC: U.S. Department of Energy, Office of Energy Efficiency and Renewable Energy. 2003. http://www.eere.energy.gov/hydrogenandfuelcells/hydrogen/production.html.

[5] J. Ogden. Where Will Hydrogen Come From? System Considerations and Hydrogen Supply. The Hydrogen Energy Transition. 73-92. Elsevier. 2004.

[6] R. Doctor, and J. Molburg. Clean Hydrogen from Coal with CO_2 Capture and Sequestration. The Hydrogen Energy Transition. 93-104. Elsevier. 2004.

[7] General Motors Corp., Argonne National Laboratory, BP, ExxonMobil, and Shell. Well-to-Wheels Engergy Use and Greenhouse Gas Emissions of Advanced Fuel/Vehicle Systems: North America Analysis. Executive Summary Report. April 2001. http://www.transportation.anl.gov/pdfs/TA/163.pdf

[8] Thomas, C. E., I. F. Kuhn, B. D. James, F. D. Lomax, and G. N. Baum. Affordable Hydrogen Supply Pathways for Fuel Cell Vehicles. *Energy.* 23. 1998.

[9] Thomas, E. E., B. D. James, F. D. Lomax, and I. F. Kuhn. Draft Final Report, Integrated Analysis of Hydrogen Passenger Vehicle Pathways. Reported to the

National Renewable Energy Laboratory, Under Subcontract No. AXE-6-16685-01. Golden CO: US Department of Energy. March 1998.

[10] Wang, M. Fuel Choices for Fuel Cell Vehicles: Well-to-Wheels Energy and Emission Impacts. *Journal of Power Sources.* 112: 3017-321. 2002.

[11] Wang, M. Q. Greet 1.5- Transportation Fuel-Cycle Modle 1 Methodology Department, Use and Results, Report No. ANL/ESD-40. Center for Transportation Research, Argonne National Laboratory, prepared for the Office of Transportation Technologies, U.S. Department of Energy. Washington DC. December 1999.

[12] Weiss, M., J. Heywood, E. Drake, A. Schafer, and F. AuYeung. On the Road in 2020. MIT Energy Laboratory Report # MIT EL 00-003. Cambridge, MA: Massachusetts Institute of Tecnology . October 2000.

[13] Lyons. Hydrogen-Manufacture. Kirk-Othmer Encyclopedia of Chemical Technology, 4th ed., Vol. 13. New York: Wiley & Sons, 1995: 838-894.

[14] U.S. Department of Energy, Office of Fossil Energy, National Energy Technology Laboratory, FutureGen. 2002. http://www.netl.doe.gov/coalpower/sequestration/futureGen/main.html.

[15] White House. White House press release. February 27, 2003. http://www.whitehouse.gov/news/releases/2003/02/20030227-11.html.

[16] C. Schroeder. Hydrogen from Electrolysis. The Hydrogen Energy Transition. 120-133. Elsevier. 2004.

[17] Davidson, Keay. Road to hydrogen cars may not be so clean Environmental peril in making, containing fuel Road to hydrogen cars may not be so clean Environmental peril in making, containing fuel. San Francisco Chronicle 12/20/2004.

[18] Cortright, R.D., R.R. Davda, J.A. Dumesic, "Hydrogen from catalytic reforming of biomass-derived hydrocarbons in liquid water." *Nature* 418(2002) 964.

[19] Garcia, L., R. French, S. Czernik, E. Chronet, "Catalytic steam reforming of bio-oils for the production of hydrogen: effects of catalyst composition." *Appl. Catal. A-General* 201(2000) 225.

[20] Ghirardi, M.L., J.P. Zhang, J.W. Lee, T. Flynn, M. Seibert, E. Greenbaum, A. Melis, "Microalgae: a green source of renewable H-2." *Trends Biontech.* 18(2000) 506.

[21] Sun, Q., Y.C. Tang, G.R. Gavalas, "Methane pyrolysis in a hot filament reactor." *Energy Fuel.* 14(2000) 490.

[22] Li, L., R.W. Borry, E. Iglesia, "Reaction-transport simulation of non-oxidative methane conversion with continuous hydrogen removal – homogeneous-heterogeneous reaction pathways." *Chem. Eng. Sci.* 56(2001) 1869.

[23] Czernik, S. R., C. French, E. Chomel. Production of Hydrogen from Biomass by Pyrolysis/steam Reforming. Advances in Hydrogen Energy. 2000.

[24] Choudhary, T.V., E. Aksoylu, D.W. Goodman, "Nonoxidative activation of methane." *Catal. Rev.* 45(2003) 151.

[25] X. Gu, J. Zhang, J. Dong, T.M. Nenoff, A Platinum-Cobalt-Loaded NaY Zeolite Membrane for Nonoxidative Conversion of Methane to Higher Hydrocarbons and Hydrogen. *Catal. Lett*., 102, 1-2 (2005), 9 – 13.

[26] Midilli, A., M. Dogru, G. Akay, C. R. Howarth. Hydrogen Production from Sewage Sludge via a Fixed Bed Gasifier Product Gas. *Internation Journal of Hydrogen Energy* 27 (2002).

[27] Rogers, R. Hydrogen Production by Gasification of Municipal Solid Waste. Lawrence Livermore National Laboratory. 1994, UCRL-ID-117603.

[28] Miyake, J., T. N. Veziroglu, and P. K. Takashashi. Hydrogen Engergy Progress VIII. Proceedings 8th WHEC. Hawaii, Pergamon Press, New York. 1990.

[29] Nath, K., D. Das. Hydrogen from Biomass. Current Science 85. 2003.

[30] Shabaker, J.W., G. W. Huber, R.R. Davda, R. D. Cortright, and J.A. Dumesic. Aqueous-phase Reforming of Ethylene Glycol over Supported Platinum Catalysts. Catalysis Letters 88. 2003.

[31] Navarro, R. M., M.C. Alvarez-Galvan, M. Cruz Sanchez-Sanchez, F. Rosa, J. L. G. Fierro. Production of Hydrogen by Oxicative Reforming of Ethanol over Pt Catalysts Supported on Al_2O_3 modified with Ce and La. *Applied Catalysis B: Environmental* 55. 2005.

[32] Shabaker, J. W., G. W. Huber, J. A. Dumesic. Aqueous-phase Reforming of Oxygenated Hydrocarbons over Sn-modified Ni Catalysts. *Journal of Catalysis* 222. 2004.

[33] Davda, R. R., J. W. Shabaker, G. W. Huber, R. D. Cortright, J. A. Dumesic. Aqueous-phase Reforming of Ethylene Glycol on Silica-supported Metal Catalysts. *Applied Catalysis B: Environmental* 43. 2003.

[34] J. W. Shabaker et. al. Aqueous-phase reforming of methanol and ethylene glycol over alumina-supported platinum catalysts. *Journal of Catalysis*. Vol. 215. 344-352.

[35] G.M. Lu, T. Hoffer, L. Guczi, Reducibility and CO Hydrogenation over Pt and Pt-CO Bimetallic Catalysts Encaged in NaY-zeolite. *Catal. Lett*. Vol. 14 (1992) 207.

[36] E. Yoldas. Alumina sol preparation from alkoxides Ceramic. Bulletine. Vol. 54. (1975) 289.

[37] X. Gu, J. Dong, T.M. Nenoff, Synthesis of defect-free FAU-type zeolite membranes and separation for dry and moist CO2/N2 mixtures. *Ind. Eng. Chem. Res.*, 44 (2005), 937 – 944]

[38] J. McMurry, R.C. Fay, Chemistry, 3rd ed., Prentice-Hall, 2001.

[39] G. Lelong, D. L. Price, A. Douy, S. Kline, J. W. Brady, M.L. Saboungi, Molecular dynamics of confined glucose solutions, *J. Chem. Phys*, 122, 2005.

DISTRIBUTION LIST

Justin Monroe
New Mexico Institute of Mining and Technology
Department of Materials and Metallurgical Engineering
801 Leroy Place
Socorro, NM 87801-4796

Daniel H. Doughty
Sion Power
9040 South Rita Road
Tucson, AZ 85747-9108

3	MS0123	Donna L. Chavez, 01011
1	MS0512	Thomas E. Blejwas, 02500
1	MS0613	Michael R. Prairie, 02520
1	MS0614	Thomas F. Wunsch, 02521
1	MS0614	David Ingersoll, 02521
1	MS0614	Karen E. Waldrip, 02521
1	MS0614	Terrence L. Aselage, 02522
1	MS0614	Judolph G. Jungst, 02523
1	MS1130	Deidre A. Hirschfeld, 01813
2	MS9018	Central Technical Files, 08944
2	MS0899	Technical Library, 04536